Applied Clay Science 104 (2015) 221–228

Contents lists available at ScienceDirect

Applied Clay Science

journal homepage: www.elsevier.com/locate/clay

Research paper

CO_2 capture by kaolinite and its adsorption mechanism

Yen-Hua Chen *, De-Long Lu

Department of Earth Sciences, National Cheng Kung University, Tainan 701, Taiwan

ARTICLE INFO

Article history:
Received 14 May 2014
Received in revised form 17 November 2014
Accepted 28 November 2014
Available online 13 December 2014

Keywords:
Kaolinite
Acid treatment
CO_2 capture
Adsorption mechanism

ABSTRACT

The low-cost and naturally abundant clay mineral kaolinite was studied for use an adsorbent for CO_2 capture. Samples of kaolinite were subjected to acid treatments to improve their textural properties, namely, its surface area and pore volume. It was found that the kaolinite sample treated with 3 M H_2SO_4 for 10 h reaction exhibited the highest Brunauer–Emmett–Teller (BET) surface area (18.9–74.3 m^2/g) and pore volume (0.11–0.31 cm^3/g). The CO_2 adsorption capacity of kaolinite, which was ~0 mg-CO_2/g-sorbent at 25 °C, increased to 3.4 mg-CO_2/g-sorbent after the acid treatment. Moreover, it was found that the CO_2 adsorption capacity of kaolinite was greater at room temperature than at higher temperatures. The CO_2 adsorption by kaolinite, which was investigated using X-ray diffraction analysis, Fourier transform infrared spectroscopy, and CO_2 adsorption isotherm measurements, was found to be mainly attributable to physical adsorption.

1. Introduction

Global warming due to CO_2 emissions into the atmosphere has become a public concern and an important environmental challenge facing the world (Rosa and Ribeiro, 2001; Damen et al., 2006; Gibbins and Chalmers, 2008). One potential solution is to develop and implement CO_2 capture and storage (CCS) technologies. Adsorption is considered to be a promising CCS technology for separating CO_2 from gas mixtures owing to its low energy requirement, ease of implementation, and low maintenance. A number of novel CO_2 adsorbents are being studied, and considerable attention is been paid to mesoporous silicas because of their large surface areas, uniform mesopores, and tunable pore size (Peter and Sayari, 2006; Son et al., 2008; Du et al., 2013). Mello et al. (2011) reported that MCM-41 exhibits a CO_2 adsorption capacity of 5.3 mg/g. Sanz et al. (2012) studied the adsorption and desorption of CO_2 on SBA-15 and reported that its CO_2 adsorption capacity was 19.4 mg/g at 298 K. Xu et al. (2002) developed a functional MCM-41 material that exhibited a CO_2 adsorption capacity as high as 133 mg/g. However, the above-mentioned materials are expensive and therefore hard to adopt on an industrial scale.

A number of alternatives, including basic liquid-form sorbents and supported amines (MacDowell et al., 2010; Choi et al., 2011; Nuchitprasittichai and Cremaschi, 2011; Brilman et al., 2013), are being considered. Nonetheless, the need for the thermal regeneration of the adsorbent results in issues such as adsorbent decomposition and increased energy consumption. A new approach should consist in the preparation of regenerable materials with lower basicities, able to achieve simultaneous retention of large amounts of CO_2 with easy release upon slight heating. In this regard, clay minerals (Venaruzzo et al., 2002; Rodlert et al., 2004; Gil et al., 2009) appear to be the most suitable materials owing to their low basicities. Clay mineral is one of the most abundant natural materials and is thus available at a low cost. For example, kaolinite, a clay mineral, consists of tetrahedral silicate sheets and octahedral hydroxide sheets in a 1:1 ratio (Deng et al., 2002; Sperinck et al., 2011). Thus, clay mineral can be a potential CO_2 adsorbent owing to its low cost, rich natural abundance, and high mechanical and chemical stability. Consequently, clay mineral should exhibit significant potential for use in the adsorption and separation of CO_2. Yet few studies have investigated the suitability of acid-treated clay minerals for CO_2 capture or their adsorption mechanism.

From an industrial point of view, most research efforts have focused on clay minerals. In this study, the commonly available and cheap clay mineral kaolinite was investigated for use as a CO_2 adsorbent. It was treated with H_2SO_4 in order to improve its textural properties, namely, its pore volume and surface area, for CO_2 capture. The acid-treated adsorbent sample was compared with the untreated one. Next, the acid-treated sample was used for CO_2 adsorption, which was characterized using thermogravimetric analysis (TGA). The crystal structure, textural properties, and morphology of the adsorbent were characterized using X-ray diffraction (XRD) analysis, N_2 adsorption tests (i.e., Brunauer–Emmett–Teller or BET measurements), and scanning electron microscopy (SEM). The effects of the pretreatment temperature and time (i.e., of the treatment before CO_2 adsorption), the adsorption temperature, and the desorption temperature on the CO_2 adsorption–desorption process as well as the thermal stability of kaolinite were investigated. Further, we attempted to determine whether acid-treated kaolinite exhibited a higher CO_2 adsorption capacity than did untreated kaolinite. We also investigated whether the adsorption of CO_2 onto kaolinite was owing to physical adsorption or whether it also involved chemical adsorption.

* Corresponding author. Tel.: +886 62 757575x65420; fax: +886 62 740285.
E-mail address: yhc513@mail.ncku.edu.tw (Y.-H. Chen).

http://dx.doi.org/10.1016/j.clay.2014.11.036
0169-1317/

Therefore, the adsorption mechanism of kaolinite was studied in depth using XRD analysis, Fourier transform infrared (FTIR) spectroscopy, and CO_2 adsorption isotherm measurement.

2. Materials and methods

2.1. Preparation of acid-treated kaolinite

In order to improve the textural properties, pore volume, and surface area of kaolinite, kaolinite samples purchased from San-Lin company (Taipei, Taiwan) were treated with H_2SO_4 solutions of different concentrations (0.5, 1, 2, and 3 M). Kaolinite was added to the acid solution in a fixed ratio of 1 g of kaolinite per 10 ml of acid. Next, the mixtures were heated in a bath at 95 °C for the acid treatment, while being stirred at 300 rpm for 3, 5, 10, and 15 h. Next, the dispersions were filtered and the precipitates were washed with large amounts of deionized water and dried in an oven overnight at 60 °C. The H_2SO_4 solution concentration of 3 M was found to be the most suitable one, as it resulted in the highest pore volume and surface area. The textural properties of the various kaolinite samples treated with the H_2SO_4 solutions of different concentrations and for various reaction times are listed in the Tables 1 and 2, respectively.

2.2. Characterization of acid-treated kaolinite

The crystal structure of kaolinite was identified using XRD analysis. The morphology and the grain distribution of kaolinite were observed using SEM. To study the thermal stability of the kaolinite, TGA was performed using a NETZSCH analyzer. The sample was ground into a powder and analyzed over temperatures of 25–1000 °C at a heating rate of 10 °C/min in a N_2 atmosphere. The textural properties of kaolinite were characterized on the basis of physical adsorption of N_2 at 77 K. A Micromeritics ASAP 2020 analyzer was employed for the purpose. The acid-treated kaolinite sample was degassed at 150 °C under vacuum for 24 h before the measurement. The surface area was determined from the N_2 adsorption isotherm using the BET equation. The total pore volume was calculated on the basis of the amount of N_2 absorbed after the completion of pore condensation; the relative pressure (P/P_0) was 0.995. The pore sizes were determined from the Barrett–Joyner–Halenda (BJH) pore size distribution curve.

2.3. Determination of CO_2 adsorption capacity

The CO_2 adsorption–desorption performance of the acid-treated kaolinite sample was assessed on the basis of the changes in its weight resulting from the adsorption and desorption of pure CO_2; the changes were determined from the results of TGA. Approximately 10 mg of the sorbent was placed in the measuring pan, and the temperature was increased from 25 °C to the desired temperature (150, 200, and 250 °C) at a rate of 10 °C/min. The sample was then heated at the desired temperature for 40, 80, 120, and 180 min in pure N_2 (99.9%), whose flow rate was 100 ml/min, in order to remove moisture and other impurities from the sample. The temperature was then dropped to the desired adsorption temperature (25, 50, 100, and 150 °C), and the flowing gas was changed from N_2 to pure CO_2 (99.5%). The adsorption temperature was maintained for 1 h to allow for CO_2 adsorption. Finally, the temperature was increased to 100 or 150 °C, and the flowing gas was changed back to N_2 to allow for CO_2 desorption. Then, on the basis of the change in the weight of the sample, measured using TGA, the CO_2 adsorption capacity (mg-CO_2/g-adsorbent) of the sample was calculated. It should be pointed out that the adsorption capacity as determined from the TGA results in this study is not the equilibrium adsorption capacity, as the weight of the sample kept slowly increasing even after 1 h of adsorption, most likely owing to the adsorption rate being low.

In order to elucidate the CO_2 adsorption mechanism of kaolinite (i.e., to determine the ratio of the amounts of CO_2 adsorbed physically and chemically), its CO_2 adsorption isotherm at 298 K was also determined using an ASAP 2020c (Micromeritics) static volumetric apparatus. As the CO_2 adsorption isotherm was measured (this curve included physical and chemical adsorption of CO_2), desorption was performed on the sample at 25 °C for 1 h in a vacuum generated using a turbomolecular pump (to desorb the CO_2 molecules with the physical adsorption). Then the CO_2 adsorption isotherm was measured again to obtain the solely physical adsorption curve by using the ASAP 2020 analyzer. After the CO_2 adsorption experiment, the resultant was examined using XRD and FTIR analyses.

Table 1
The BET surface area, pore volume, and pore size of the kaolinites treated with H_2SO_4 solutions of different concentrations.

Concentration of H_2SO_4 (M)	BET surface area (m^2/g)	Pore volume (cm^3/g)	Pore size (nm)
0 (untreated kaolinite)	18.9	0.110	21.0
0.5	24.7	0.097	16.5
1	33.7	0.117	16.1
2	43.3	0.120	12.8
3	42.4	0.139	13.7

Table 2
The BET surface area, pore volume, and pore size of the kaolinites treated with 3 M H_2SO_4 for different treatment times.

Reaction time (h)	BET surface area (m^2/g)	Pore volume (cm^3/g)	Pore size (nm)
3	42.4	0.139	13.7
5	61.0	0.164	11.9
10	74.3	0.305	15.3
15	77.6	0.290	17.8

3. Results and discussion

3.1. Characteristics of untreated kaolinites

The XRD pattern of the untreated kaolinite sample is shown in Fig. 1(a). The diffraction peaks could be attributed as belonging to kaolinite with a triclinic structure and were in agreement with the standard data given in its ICDD card (58–2001). No impurity peaks were observed. Further, the intensity of the diffraction peaks was high and the peaks were sharp. This indicated that the starting sample was highly crystalline and consisted entirely of kaolinite. Moreover, the XRD pattern of acid-treated kaolinite kept unchanged after acid treatment (Fig. 1(b)), which suggested the structure of kaolinites would not be affected with acid treatment.

The morphology of the kaolinite sample was investigated using SEM; the resulting image is shown in Fig. 2(a). It can be seen that the kaolinite sample was composed of large as well as small grains. The former

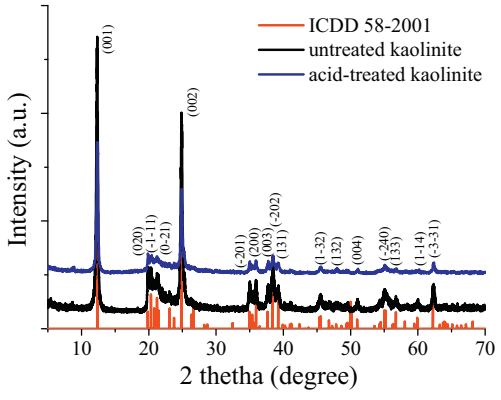

Fig. 1. The XRD pattern of the untreated and acid-treated kaolinites.

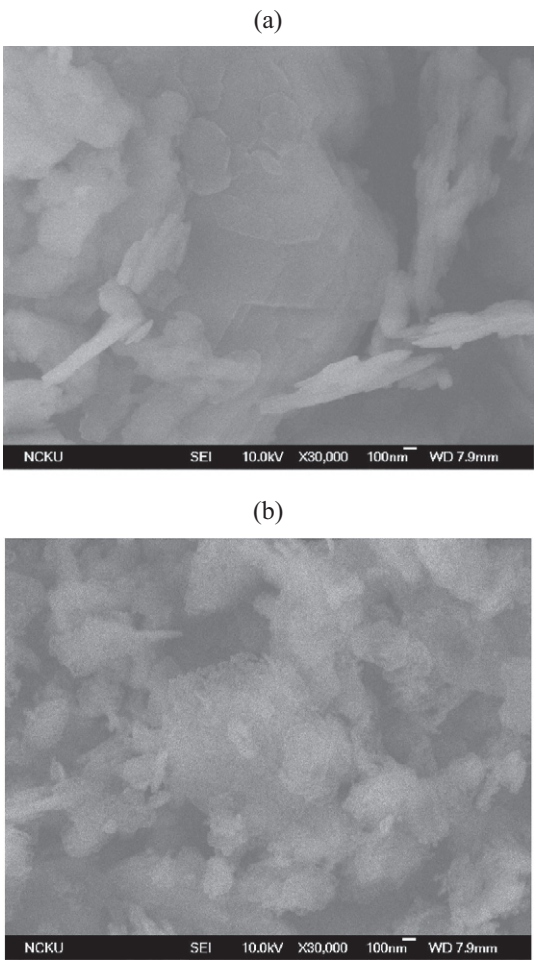

Fig. 2. The SEM morphologies of the (a) untreated and (b) acid-treated kaolinites.

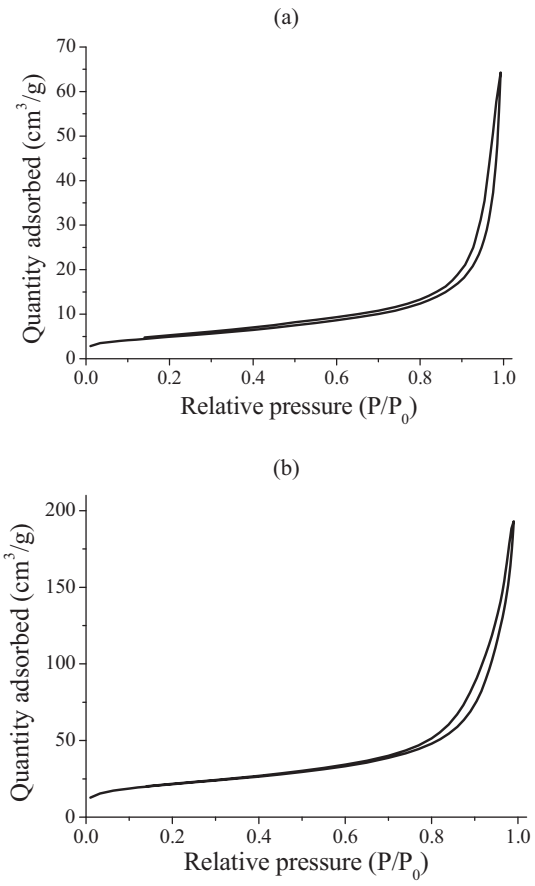

Fig. 3. The nitrogen adsorption–desorption isotherm curves for the (a) untreated and (b) acid-treated kaolinites.

had a hexagonal shape with a layered-stacking structure and their size was approximately 5 μm, while the latter had a fracture-like shape. The smaller grains formed aggregates that had a diameter of approximately 1 μm. The SEM image of acid-treated kaolinite showed an uneven and cracked surface (Fig. 2(b)); it indicated a more rough and fractured surface made the acid-treated kaolinite along with a higher surface area after acid treatment.

The specific surface area, pore volume, and pore diameter of the kaolinite sample were 18.9 m^2/g, 0.11 cm^3/g, and 21.0 nm, respectively. The N_2 adsorption–desorption isotherm curve for the kaolinite sample is shown in Fig. 3(a). On the basis of the IUPAC classification, the isotherm could be labeled as a typical type-IV isotherm (Miller et al., 1987) because it exhibited a hysteresis loop between the adsorption and desorption curves. Moreover, the shapes of the adsorption and desorption curves were similar to that of an H3 hysteresis loop (Leslie-Pelecky and Rieke, 1996). This type of an isotherm is usually noticed in the case of aggregates of tabular or sheet-like materials and was thus indicative of the layer-like structure of the kaolinite sample.

3.2. Characterization of acid-treated kaolinite

3.2.1. Effects of acid treatment on the textural properties of kaolinite

To improve the textural properties of kaolinite, samples of the adsorbent were treated with H_2SO_4 solutions with concentrations of 0.5, 1, 2, and 3 M. Table 1 lists the textural properties, including the BET surface areas, pore volumes, and pore sizes, of the untreated and treated kaolinite samples. The surface area and pore volume of the untreated kaolinite sample were 18.9 m^2/g and 0.11 cm^3/g, respectively, indicating that the original kaolinite exhibited low porosity. After the acid treatment, the values increased to 42.4 m^2/g and 0.139 cm^3/g, respectively. This suggested that an acid treatment can effectively improve the textural properties of kaolinite. This is probably owing to the dissolution of the metal ions present in the kaolinite and the rearrangement of its crystal structure, as a result of a reaction between the acid and the clay mineral.

Of the various acid-treated kaolinite samples, the one treated with the 3 M solution of H_2SO_4 exhibited the highest pore volume and surface area and was thus selected to study the effects of the treatment time (3, 5, 10, and 15 h) on the textural properties. Table 2 lists the textural properties of the kaolinite samples treated with the 3 M solution of H_2SO_4 for different treatment times. It can be seen that the surface area and pore volume of the kaolinite sample increased with an increase in the reaction time. For reaction times of 10 and 15 h, the surface areas were 74.3 and 77.6 m^2/g, respectively, while the pore volumes were 0.305 and 0.290 cm^3/g, respectively. Thus, because of energy and cost considerations, we used the kaolinite sample treated with the 3 M solution of H_2SO_4 for 10 h for CO_2 capture and its N_2 adsorption–desorption isotherm curve was shown in Fig. 3(b). The isotherm curve could be labeled as a typical type-IV isotherm and an H3 hysteresis loop.

3.2.2. Thermal stability of acid-treated kaolinite

The thermal stability of acid-treated kaolinite was measured through TGA and differential thermal analysis (DTA). The variation of weight for the kaolinite sample and the corresponding derivative thermogravimetric (DTG) and DTA curves are shown in the Fig. 4. The acid-treated kaolinite sample exhibited a weight loss of 4.5% at 455 °C, as evidenced by the DTG curve peak at 500 °C, while the DTA curve showed an endothermic peak at approximately 575 °C. This weight loss was related to the dehydroxylation of the kaolinite layers. This

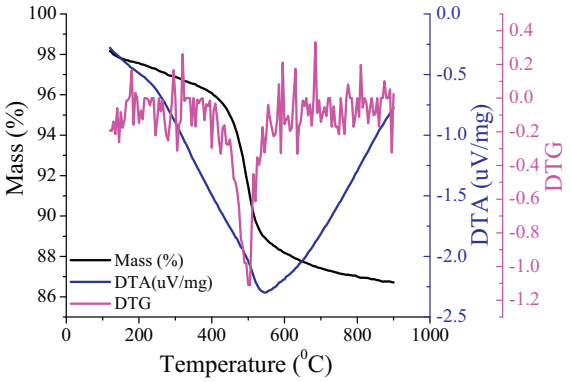

Fig. 4. The weight loss and corresponding first derivative DTG curve and DTA curve of acid-treated kaolinite.

result was in keeping with those reported previously (Piga, 1995; Cheng et al., 2010; Ptáček et al., 2010). On the basis of these results, the temperature was kept at less than 455 °C when investigating the CO_2 adsorption–desorption mechanism of kaolinite.

3.3. Results of CO_2 adsorption analysis

The CO_2 adsorption capacities of the untreated and acid-treated kaolinite samples were examined. However, because the CO_2 adsorption capacity of the untreated samples was lower than the detection limit of the TGA system employed, we will focus on the kaolinite sample treated with 3 M H_2SO_4 for 10 h. It is known that the pretreatment temperature and time as well as the adsorption and desorption temperatures have significant effects on the adsorption capacity of an adsorbent. We now discuss how these factors affected the adsorption of CO_2 by kaolinite.

3.3.1. Effect of the pretreatment temperature

Before determining the CO_2 adsorption capacity, the pretreatment temperature of the kaolinite sample was increased from 25 °C to the desired level (150, 200, and 250 °C). The results of the CO_2 adsorption capacity measurement are shown in Fig. 5. It can be seen that a weight loss of approximately 2% occurred during the pretreatment process, owing to the desorption of the physically adsorbed water. This was followed by an increase in weight because of the adsorption of CO_2. The CO_2 adsorption capacity of kaolinite was determined using the following formula: Q (capacity in mg/g) = ((the weight of the sample after CO_2 adsorption) − (the weight of the sample before CO_2 adsorption)) / (the weight of the sample before CO_2 adsorption). From the TG curve, the CO_2 adsorption capacities for pretreatment temperatures of 150, 200, and 250 °C were found to be 2.8, 2.7, and 2.5 mg/g, respectively. The CO_2 adsorption capacities at the three temperatures were almost the same. Therefore, in order to save time and energy, we chose 150 °C as the pretreatment temperature for the rest of the study.

3.3.2. Effect of pretreatment time

Next, before determining the CO_2 adsorption capacity, the sample was heated to 150 °C and held at this temperature for 40, 80, 120, and 180 min in a flow of pure N_2. The results of the CO_2 adsorption capacity measurement are shown in Fig. 6. It can be seen that the curve is unstable in the high-temperature region; this was owing to deviations in the TGA system used for the measurements. From the TG curve, the CO_2 adsorption capacities were calculated to be 3.3, 3.2, 3.0, and 3.5 mg/g for pretreatment times of 40, 80, 120, and 180 min, respectively. Thus, the CO_2 adsorption capacities corresponding to the different pretreatment times were almost the same, suggesting that the pretreatment times investigated were enough to allow all the physically adsorbed water to be fully desorbed. Therefore, in order to save time and energy, the pretreatment time was set at 40 min.

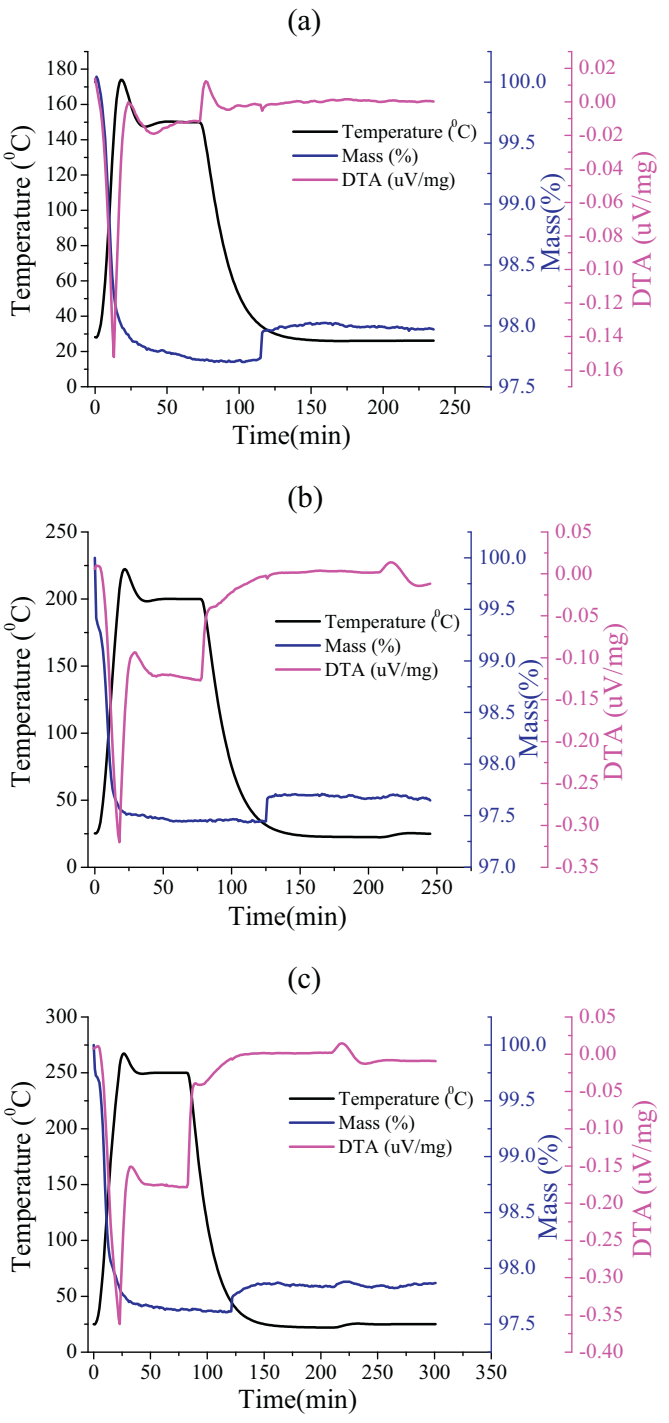

Fig. 5. The CO_2 adsorption capacity in relation to the pre-treated temperature of acid-treated kaolinite from the TG measurement at (a) 150, (b) 200, and (c) 250 °C.

3.3.3. Effect of temperature during adsorption

In order to evaluate the temperature effect during CO_2 adsorption, the sample was held at the temperatures of 25, 50, 100, and 150 °C for 2 h to allow for CO_2 adsorption. The results of the CO_2 adsorption capacity measurement are shown in Fig. 7. It can be seen that the CO_2 adsorption capacity of kaolinite decreased with an increase in the adsorption temperature. The CO_2 adsorption capacities were 3.3, 2.4, 0, and 0 mg/g for adsorption temperatures of 25, 50, 100, and 150 °C, respectively. Thus,

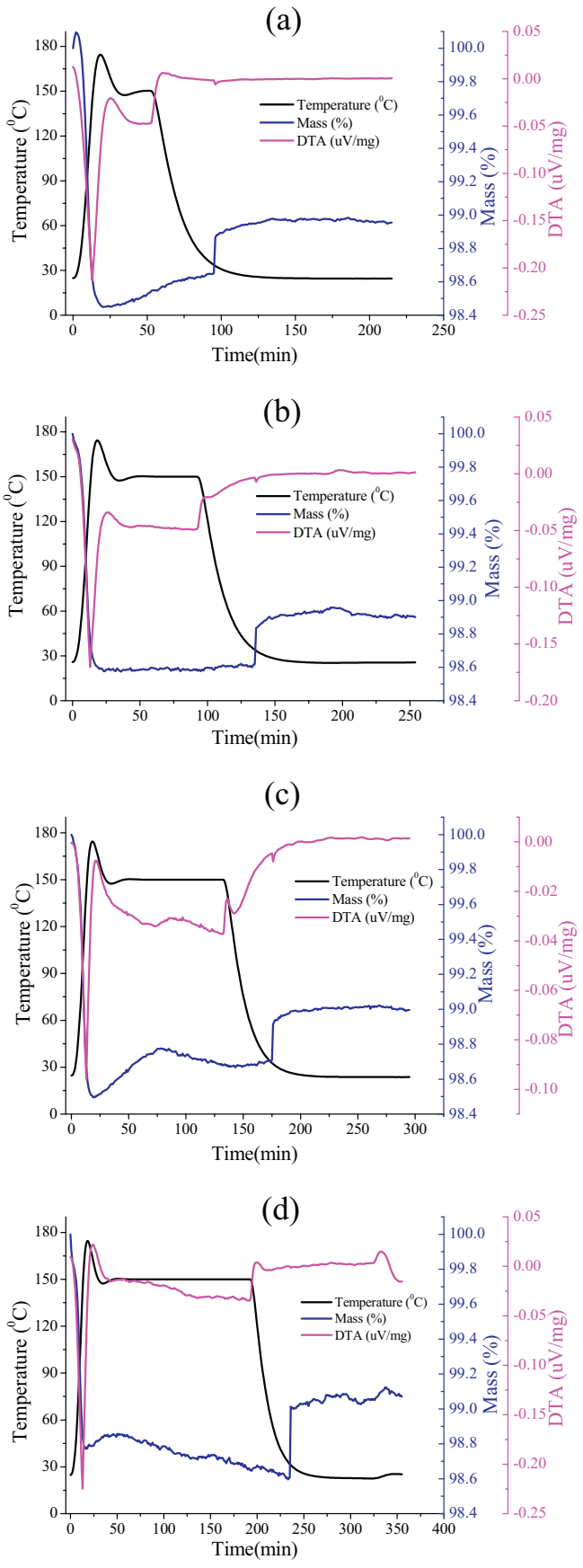

Fig. 6. The CO_2 adsorption ability and the pre-treated time of (a) 40, (b) 80, (c) 120, and (d) 180 min for the acid-treated kaolinite from the TG measurement.

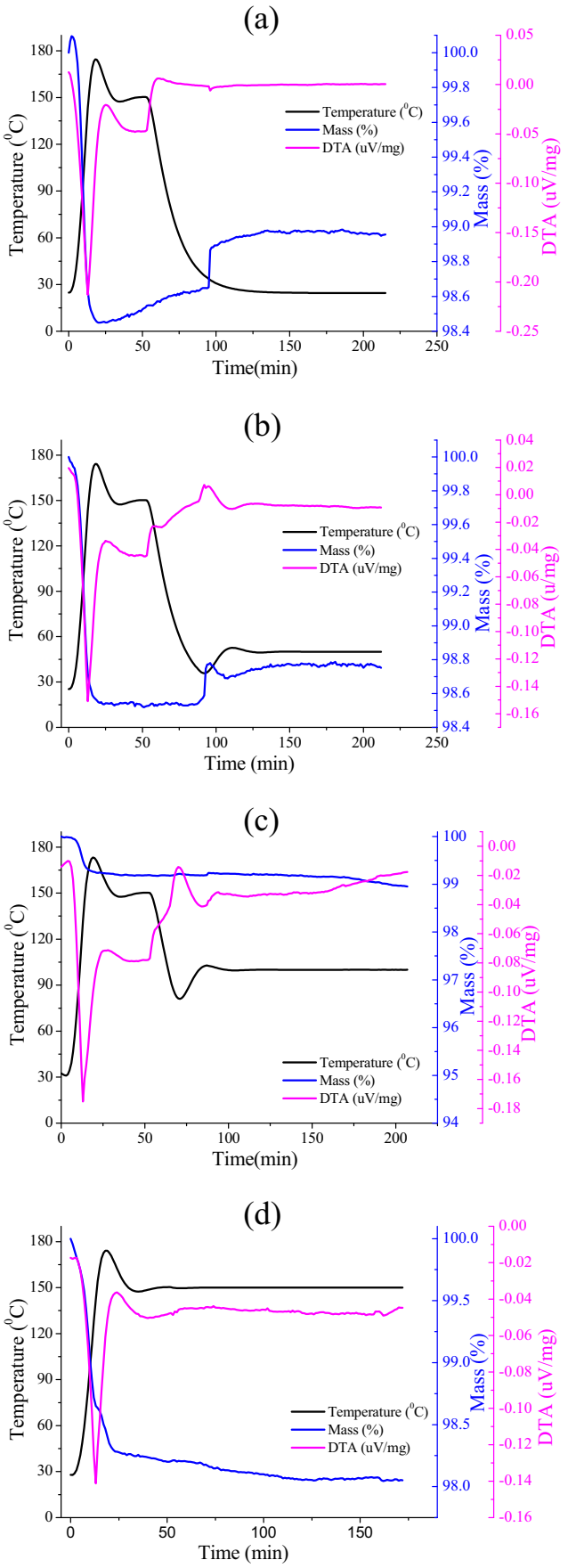

Fig. 7. The CO_2 adsorption capacity in relation to the adsorption temperatures of (a) 25, (b) 50, (c) 100, and (d) 150 °C by the TG measurement.

the ideal CO_2 adsorption temperature was determined to be 25 °C, as it resulted in the highest CO_2 adsorption capacity.

3.3.4. Effect of desorption temperature

CO_2 was made to desorb from the kaolinite sample using the following procedure. The temperature was kept at 100 or 150 °C, and the sample was held at the chosen temperature for 1 h in a flow of pure N_2 to allow for CO_2 desorption. The result is shown in Fig. 8. It can be observed that the sample still exhibited a little bit weight gain at the desorption temperature of 100 °C, as evidenced by the TG curve peak. This means the mass all the adsorbed CO_2 desorbed at 150 °C but not at 100 °C, which suggests the adsorbed CO_2 molecules cannot be completely desorbed at the temperature of 100 °C. Therefore, the ideal desorption temperature for completely removing the adsorbed CO_2 gas was determined to 150 °C.

3.4. Analyses of kaolinite after CO_2 adsorption

3.4.1. XRD analysis

The XRD pattern of the acid-treated kaolinite sample obtained after CO_2 adsorption was the same as that before CO_2 adsorption, suggesting that no new diffraction peaks were noticed after the adsorption of CO_2. Usually, when CO_2 molecules enter the interlayer spaces of kaolinite, the d-spacing of the (001) plane should increase. However, the position of the (001) plane peak did not change, indicating that the interlayer spacing remained almost the same. We believe that this was because there may be no amount of CO_2 entering the interlayer spaces of the kaolinite sample, resulting in a negligible increase in the spacing.

3.4.2. FTIR analysis

The FTIR spectrum of the acid-treated kaolinite sample is shown in Fig. 9. The triclinic layer structure of the kaolinite sample resulted in four well-resolved (OH) bands. Three of these bands could be assigned to the stretching vibrations of the surface hydroxyl groups (3694, 3668, and 3652 cm^{-1}), while the fourth one (3620 cm^{-1}) was attributable to the vibration of the inner hydroxyl groups. The (Si-O) band exhibited three well-resolved bands in the 1000–1100 cm^{-1} region. The OH-bending region of the acid-treated kaolinite sample exhibited peaks corresponding to vibrations of the inner-surface OH groups (at 937 cm^{-1}) as well of those corresponding to the inner OH groups (near 915 cm^{-1}). Absorption bands noticed at approximately 698 and 754 cm^{-1} were associated with the Si-O vibrational modes; absorption bands due to Si-O-Al and Si-O-Si were also observed at 543 and 473 cm^{-1}, respectively. These were in agreement with the literatures (Madejova and Komadel, 2001; Georges-Ivo, 2005; Vaculikova et al., 2011; Spence and Kelleher, 2012; Aroke et al., 2013).

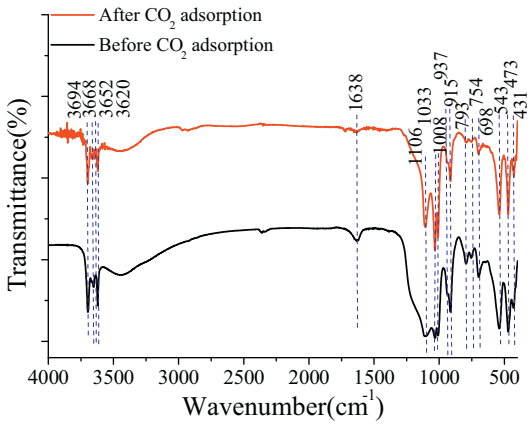

Fig. 9. The FTIR spectrum of acid-treated kaolinite before and after CO_2 adsorption.

The FTIR spectrum of the acid-treated kaolinite sample obtained after CO_2 adsorption is also shown in Fig. 9. All the previously noticed peaks were present, and no new peaks were observed. The bands attributed to carbonates, located at 813 and 690 cm^{-1} (Bhattacharyya, 1989; Christenson, 1993; Cole et al., 2010), were not observed, indicating that the adsorbed CO_2 molecules did not react with OH group to form carbonates. Because there was no strong evidence for chemical bonding (vibrational modes disappear or additional bands occur), it can be surmised that the adsorption of CO_2 onto kaolinite was mainly attributable to physical adsorption.

3.4.3. CO_2 adsorption isotherm

In order to confirm the CO_2 adsorption mechanism of kaolinite, the measurement of CO_2 adsorption isotherm was performed at 298 K by using the ASAP 2020c analyzer. The two resulting isotherm curves, which corresponded to physical and chemical adsorption, are shown in Fig. 10. The degree of chemical adsorption remained unchanged at zero for increases in the pressure. On the other hand, the degree of physical adsorption increased with an increase in the pressure, with the CO_2 adsorption capacity at a pressure of 765 mm Hg being 3.6 mg/g. This result was in keeping with those of the TG measurement (3.3 mg/g). Thus, it was confirmed again that the adsorption of CO_2 by the investigated kaolinite samples was exclusively because of physical adsorption.

3.5. CO_2 adsorption mechanism of kaolinite

Table 3 lists the CO_2 adsorption mechanisms of various clay minerals as reported in the literatures (Bhattacharyya, 1989; Christenson, 1993; Cole et al., 2010). Bhattacharyya (1989), Christenson (1993), and Cole et al. (2010) found that mica adsorbed CO_2 through the formation of a bicarbonate owing to the reaction between the CO_2 and OH groups; this bicarbonate reacts with the CO_2 and the cations of inner layers of mica. Giesting et al. (2012) reported that the CO_2 adsorption mechanism of montmorillonite was based on the reaction of CO_2 with the

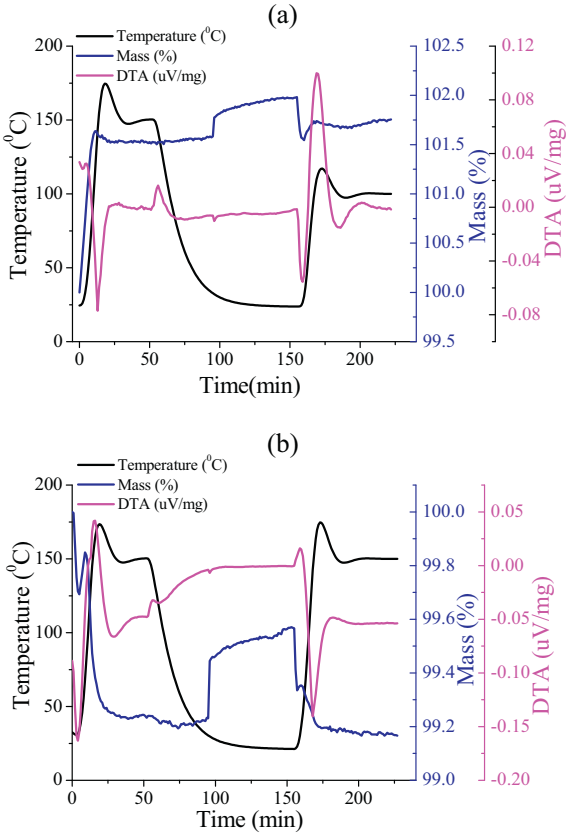

Fig. 8. The relationship between the CO_2 adsorption ability and the desorption temperatures of (a) 100 °C and (b) 150 °C from the TG measurement.

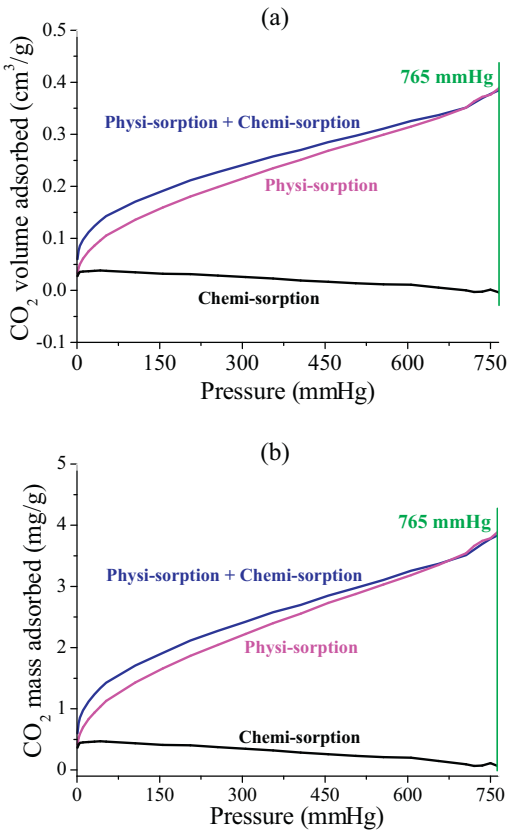

Fig. 10. The CO_2 adsorption isotherm curves of (a) untreated and (b) acid-treated kaolinites derived from the measurement by using ASAP 2020c analyzer at 25 °C.

H_2O present in montmorillonite. There are no cations present in the interlayer spaces in the kaolinite structure. Therefore, the CO_2 adsorption mechanism of kaolinite is based on the reaction of the OH group with the CO_2, resulting in the formation of a bicarbonate. However, the obtained results showed that bonds involving $–HCO_3$ were not present in the kaolinite sample that been used for CO_2 adsorption. This may have been because the amount of bicarbonate produced was very small and lower than the limited detection of the analyzers employed in the present study. To sum up, the XRD pattern, the FTIR spectrum, and the CO_2 adsorption isotherms suggested that kaolinite had not reacted with CO_2. Therefore, it was further confirmed that the adsorption of CO_2 by kaolinite is mainly owing to physical adsorption.

4. Conclusion

Kaolinite, a cheap and commonly available clay mineral, was modified by an acid (H_2SO_4) treatment. The surface area and the porosity of the acid-treated kaolinite sample were much higher than that of the untreated one. This suggested an acid treatment is an effective way of improving the textural properties of kaolinite. Moreover, the CO_2 adsorption capacity of kaolinite was also improved by the acid treatment. It was found that the adsorption of CO_2 by kaolinite is physical in nature; this conclusion was arrived at on the basis of the results of XRD analysis, FTIR, and CO_2 adsorption isotherm measurements. Thus, kaolinite shows high potential as an adsorbent for CO_2 capture.

Table 3
The list of the CO_2 adsorption mechanism of clay minerals from the literatures.

Reference	Adsorbent	Adsorption mechanism
Bhattacharyya (1989)	Mica	$-OH + CO_2 \rightarrow -HCO_3$
Christenson (1993)	Mica	Cations $+ CO_2 \rightarrow -CO_3$
Cole at al. (2010)	Muscovite	$-OH + CO_2 \rightarrow -HCO_3$
Giesting et al. (2012)	montmorillonite	$-H_2O + CO_2 \rightarrow -H_2CO_3$

Acknowledgments

The authors would like to thank Prof. Wei-The Jiang of the Department of Earth Sciences for the help with XRD measurements. We thank to Prof. Lien-Chung Hsu of the Department of Material Sciences and Engineering for the FTIR analysis. We also like to thank Miss Yu-Jin Cheng in the Lab of Mineral Science and Technology for the help with the BET measurement. We sincerely thank to the National Science Council of Taiwan for the financial support.

References

Aroke, U.O., El-Nafaty, U.A., Osha, O.A., 2013. Properties and characterization of kaolin clay from Alkaleri, north-eastern Nigeria. Int. J. Emerg. Technol. Adv. Eng. 3 (11), 387–392.
Bhattacharyya, K.G., 1989. Adsorption of carbon dioxide on mica surfaces. Langmuir 5, 1155–1162.
Brilman, W., Alba, W.G., Veneman, R., 2013. Capturing atmospheric CO_2 using supported amine sorbents for microalgae cultivation. Biomass Bioenergy 53, 39–47.
Cheng, H., Liu, Q., Yang, J., Du, X., Frost, R.L., 2010. Influencing factors on kaolinite–potassium acetate intercalation complexes. Appl. Clay Sci. 50, 476–480.
Choi, S., Gray, M.L., Jones, C.W., 2011. Amine-tethered solid adsorbents coupling high adsorption capacity and regenerability for CO_2 capture from ambient Air. ChemSusChem 4, 628–635.
Christenson, H.K., 1993. Adhesion and surface energy of mica in air and water. J. Phys. Chem. 97, 12034–12041.
Cole, D.R., Chialvo, A.A., Rother, G., Vlcek, L., Cummings, P.T., 2010. Supercritical fluid behavior at nanoscale interfaces: implications for CO_2 sequestration in geologic formations. Philos. Mag. 90, 2339–2363.
Damen, K., Troost, M.V., Faaij, A., Turkenburg, W., 2006. A comparison of electricity -and hydrogen production systems with CO_2 capture and storage. Part A: review and selection of promising conversion and capture technologies. Prog. Energy Combust. Sci. 32, 215–246.
Deng, Y., White, G.N., Dixon, J.B., 2002. Effect of structural stress on the intercalation rate of kaolinite. J. Colloid Interface Sci. 250 (2), 379–393.
Du, Y.H., Du, Z.G., Zou, W., Li, H.Q., Mi, J.G., Zhang, C., 2013. Carbon dioxide adsorbent based on rich amines loaded nano-silica. J. Colloid Interface Sci. 409, 123–128.
Georges-Ivo, E.E., 2005. Fourier transform infrared spectrophotometry and X-ray powder diffractometry as complementary techniques in characterizing clay size fraction of kaolin. J. Appl. Sci. Environ. Manag. 9 (2), 43–48.
Gibbins, J., Chalmers, H., 2008. Carbon capture and storage. Energy Policy 36, 4317–4322.
Giesting, P., Guggenheim, S., Koster Van Groos, A.F., Busch, A., 2012. Interaction of carbon dioxide with Na-exchanged montmorillonite at pressures to 640bars: implications for CO_2 sequestration. Int. J. Greenh. Gas Con. 8, 73–81.
Gil, A., Dachary, A.G., Korili, S.A., 2009. Adsorption of CO_2 as a method for the characterisation of the structure of alumina-pillared clay catalysts. Adsorption 15, 203–210.
Leslie-Pelecky, D.L., Rieke, R.D., 1996. Magnetic properties of nanostructured materials. Chem. Mater. 8, 1770–1783.
MacDowell, N., Florin, N., Buchard, A., Hallett, J., Galindo, A., Jackson, G., Adjiman, C.S., Williams, C.K., Shah, N., Fennell, P., 2010. An overview of CO_2 capture technologies. Energy Environ. Sci. 3, 1645–1669.
Madejova, J., Komadel, P., 2001. Baseline studies of the clay minerals society source clays: infrared methods. Clays Clay Minerals 49 (5), 410–432.
Mello, M.R., Phanon, D., Silveira, G.Q., Llewellyn, P.L., Ronconi, C.M., 2011. Amine-modified MCM-41 mesoporous silica for carbon dioxide capture. Microporous Mesoporous Mater. 143, 174–179.
Miller, J.S., Calabrese, J.C., Rommelmann, H., Chittipeddi, H.R., Zhang, J.H., Reiff, W.M., Epstein, A.J., 1987. Ferromagnetic behavior of $[Fe(C_5Me_5)_2]'^{+}[TCNE]'^{-}$. Structural and magnetic characterization of decamethyl ferrocenium tetracyanoethenide, $[Fe(CSMe_5)_2]'^{+}[TCNE]'^{+*}MeCN$, and decamethyl ferrocenium pentacyanopropenide, $[Fe(C,Me,).]'^{+}[C_3(CN),]^{-}$. J. Am. Chem. Soc. 109, 769–781.
Nuchitprasittichai, A., Cremaschi, S., 2011. Optimization of CO_2 capture process with aqueous amines using response surface methodology. Comput. Chem. Eng. 35, 1521–1531.
Peter, J.E., Sayari, H.A., 2006. Applications of pore-expanded mesoporous silicas. 3. Triamine silane grafting for enhanced CO_2 adsorption. Ind. Eng. Chem. Res. 45, 3248–3255.
Piga, L., 1995. Thermogravimetry of a kaolinite alunite ore. Thermochim. Acta 265, 177–187.
Ptáček, P., Kubátová, D., Havlica, J., Brandštetr, J., Šoukal, F., Opravil, T., 2010. Isothermal kinetic analysis of the thermal decomposition of kaolinite: the thermogravimetric study. Thermochim. Acta 501, 24–29.
Rodlert, M., Plummer, C.J.G., Grünbauer, H.J.M., Månson, J.A.E., 2004. Hyperbranched polymer/clay nanocomposites. Adv. Eng. Mater. 6 (9), 715–719.
Rosa, L.P., Ribeiro, S.K., 2001. The present, past, and future contributions to global warming of CO_2 emissions from fuels. Climate Change 48, 289–308.
Sanz, R., Calleja, G., Arencibia, A., Sanz-Perez, E.S., 2012. Amino functionalized mesostructured SBA-15 silica for CO_2 capture: exploring the relation between the adsorption capacity and the distribution of amino groups by TEM. Microporous Mesoporous Mater. 158, 309–317.

Son, W.J., Choi, J.S., Ahn, W.S., 2008. Adsorptive removal of carbon dioxide using polyethyleneimine-loaded mesoporous silica materials. Microporous Mesoporous Mater. 113, 31–40.
Spence, A., Kelleher, B.P., 2012. FT-IR spectroscopic analysis of kaolinite–microbial interactions. Vib. Spectrosc. 61, 151–155.
Sperinck, S., Raiteri, P., Marks, N., Wright, K., 2011. Dehydroxylation of kaolinite to metakaolin—a molecular dynamics study. J. Mater. Chem. 21, 2118–2125.
Vaculikova, L., Plevova, E., Vallova, S., Koutnik, I., 2011. Characterization and differentiation of kaolinites from selected Czech deposits infrared spectroscopy and differential thermal analysis. Acta Geodyn. Geomater. 8 (1), 59–67.
Venaruzzo, J.L., Volzone, C., Rueda, M.L., Ortiga, J., 2002. Modified bentonitic clay minerals as adsorbents of CO, CO_2 and SO_2 gases. Microporous Mesoporous Mater. 56, 73–80.
Xu, X., Andresen, J.M., Song, C., Miller, B.G., Scaroni, A.W., 2002. Preparation of novel CO_2 molecular basket of polymer modified MCM-41. Fuel Chem. 47, 67–68 (Division Preprints).